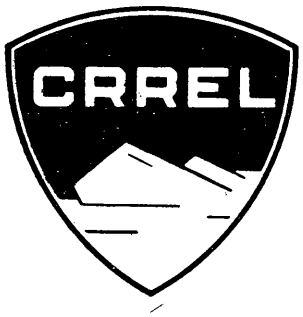

Research Report 167

ON ISOTHERMAL FLOW OF AIR INTO A PARTIALLY CASED RECTANGULAR SNOW TRENCH

by

Yin-Chao Yen

JUNE 1965

U.S. ARMY MATERIEL COMMAND
COLD REGIONS RESEARCH & ENGINEERING LABORATORY
HANOVER, NEW HAMPSHIRE

DA Task 1V014501B52A31

PREFACE

This report was prepared by Dr. Yen, Research Chemical Engineer, Materials Research Branch, Research Division.

The author wishes to thank Mr. Don Fisher for his help in setting up the computer program and obtaining the numerical result.

USA CRREL is an Army Materiel Command laboratory.

Manuscript received 16 September 1964

Department of the Army Task IV014501B52A31

CONTENTS

ILLUSTRATIONS

TABLES

SUMMARY

In a previous paper, Yen and Fisher (1963) developed an expression for evaluating the quantity of air flowing into a partly cased rectangular porous trench of constant permeability. The flow was assumed to be isothermal, steady and two-dimensional. The formula is $Q = 2(K_1'/2K_1)(k/\mu)(\rho_{avg})(p_s - p_w)$, where Q is the mass flow rate per unit length of the trench, $K_1'/2K_1$ is a configuration factor; k is permeability, μ is viscosity of air; ρ_{avg} is the average density at mean pressure; and p_s and p_w are the air pressures at the trench top and the uncased trench walls respectively. The configuration factor in this earlier work was arrived at by considering the effects of depth to the impermeable layer, d_ℓ, depth of the trench, d_t, and depth of the trench casing, d_c. In the present study, however, values of $K_1'/2K_1$ were determined which included the effect of half trench width b as well as d_ℓ, d_t and d_c. It is found that in any practical analysis the effect of trench width is not negligible and should be considered.

ON ISOTHERMAL FLOW OF AIR INTO A PARTIALLY CASED RECTANGULAR SNOW TRENCH

by

Yin-Chao Yen

Introduction

In a previous study (Yen and Fisher, 1963), an expression for mass flow rate

$$Q = 2\left(\frac{K_1'}{2K_1}\right)\left(\frac{k}{\mu}\right) <\rho_{avg}> (p_s - p_w)$$

was derived for isothermal, two-dimensional and steady flow into a covered, partially cased rectangular snow trench. In the above formula, $K_1'/2K_1$ is a configuration factor related to the depth of the impermeable layer, d_ℓ, depth of the trench, d_t, and depth of the casing, d_c. The effect of trench width was assumed to be negligible in order to simplify the mathematical analysis. The purpose of this investigation is to obtain a more accurate representation of the physical problem by including the effect of trench width in the configuration factor.

The problem

Figure 1 shows a sketch of the actual problem. It is symmetrical about the centerline of the trench. The upper portion of the trench walls is cased to an arbitrary depth, d_c. The remainder of the walls and the floor are maintained at a constant pressure that is less than the prevailing atmospheric pressure. This pressure reduction can easily be accomplished by installing a series of fans in the ceiling of the trench.

The equation of continuity for steady, Darcian flow can be written as

$$\text{Div}\,(\rho V) = 0 \qquad (1)$$

where

$$V = -\frac{k}{\mu}\,\text{grad}\,p. \qquad (2)$$

Combining eq 1 and 2 and assuming isothermal, two-dimensional flow and constant permeability, eq 1 reduces to

$$\frac{\partial^2 p^2}{\partial x^2} + \frac{\partial^2 p^2}{\partial y^2} = 0 \qquad (3)$$

with boundary conditions

$p = p_s$ at $y = d_t$, $x = -b$;

$p = p_w$ at $d_t - d_c \geqslant y \geqslant 0$, $x = -b$

and at $y = 0$, $-b \leqslant x \leqslant 0$;

$\frac{\partial p}{\partial x} = 0$ at $d_t - d_c \leqslant y \leqslant d_t$, $x = -b$;

and at $-(d_\ell - d_t) \leqslant y \leqslant 0$, $x = 0$

$\frac{\partial p}{\partial y} = 0$ at $y = -(d_\ell - d_t)$, $x \leqslant 0$.

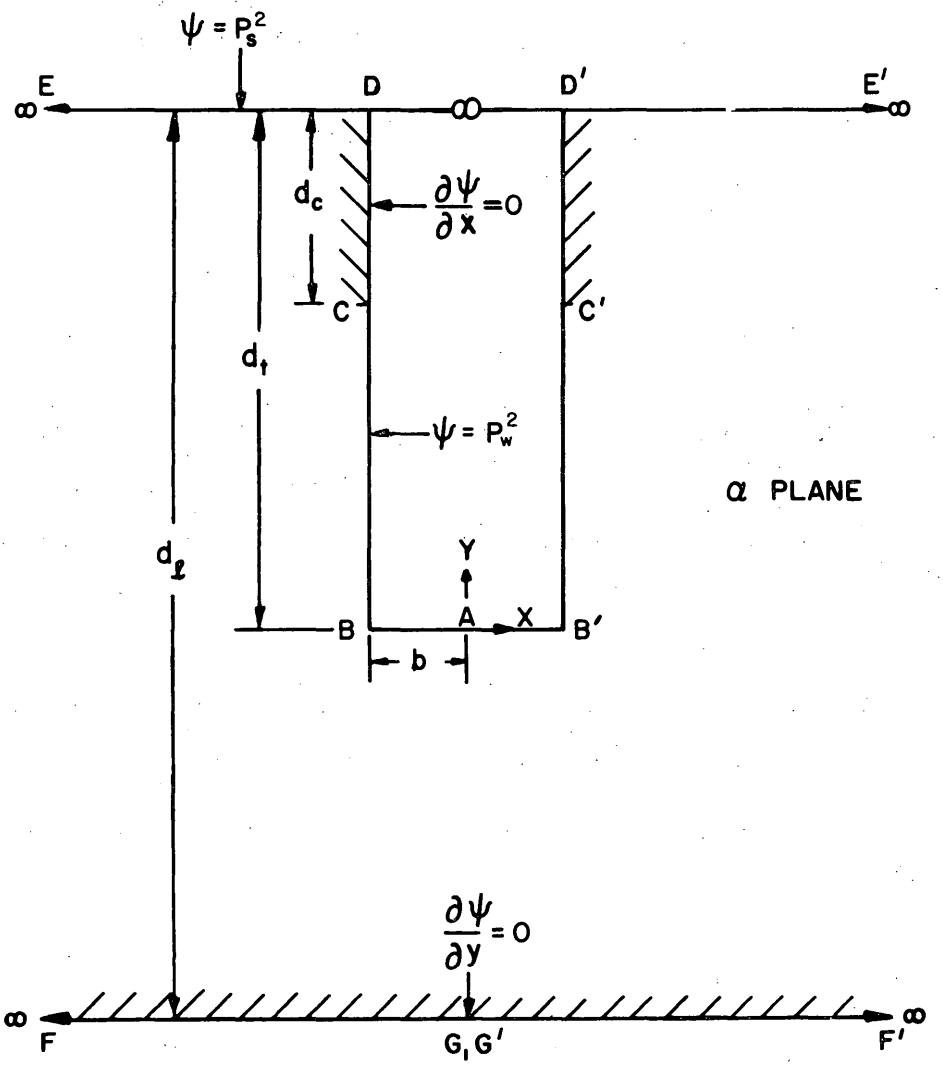

Figure 1. Sketch of the physical problem.

Equation 3 is linear in p^2 by writing $\psi = p^2$; eq 3 becomes

$$\frac{\partial^2 \psi}{\partial x^2} + \frac{\partial^2 \psi}{\partial y^2} = 0. \tag{3a}$$

The boundary conditions in terms of ψ as shown in Figure 1 are

$\psi = p_s^2$, $\quad y = d_t, \quad x = -b$

$\psi = p_w^2$, $\quad d_t - d_c \geq y \geq 0, \quad x = -b$ and $y = 0, \quad -b \leq x \leq 0$

$\frac{\partial \psi}{\partial x} = 0$, $\quad d_t - d_c \leq y \leq d_t, \quad x = -b$

$\frac{\partial \psi}{\partial x} = 0$, $\quad -(d_\ell - d_t) \leq y \leq 0, \quad x = 0$

$\frac{\partial \psi}{\partial y} = 0$, $\quad y = -(d_\ell - d_t), \quad x = 0.$

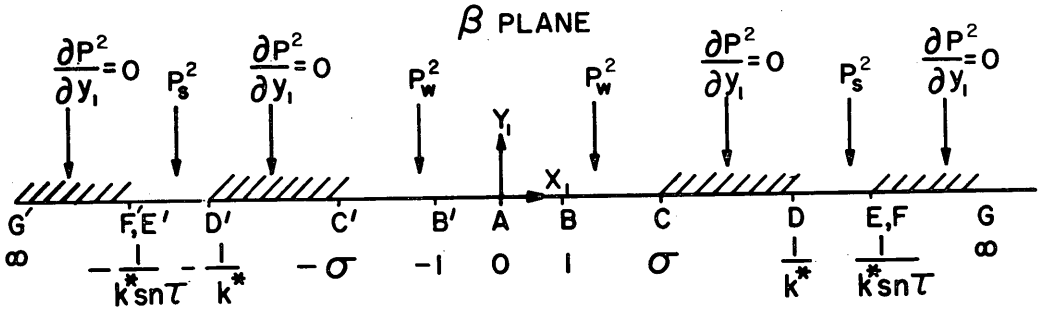

Figure 2. Figure 1 mapped into upper half of β plane.

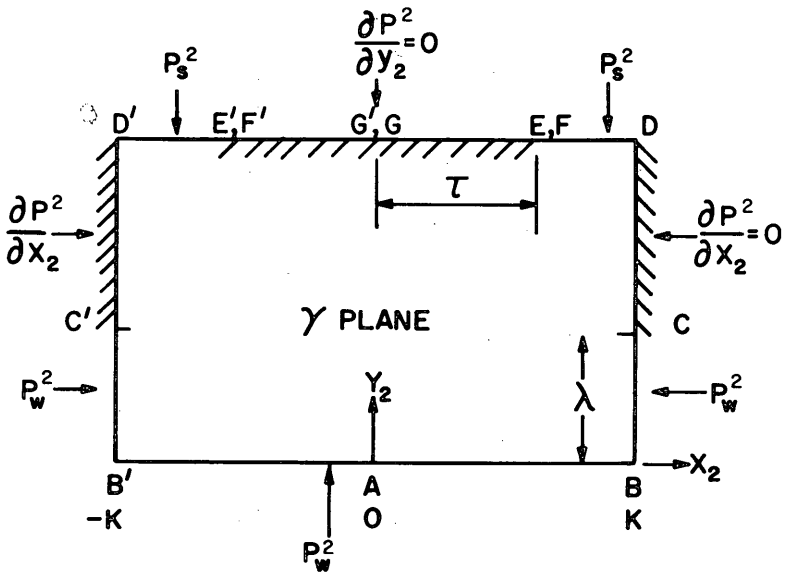

Figure 3. Upper half of β plane mapped into interior of rectangle in γ plane.

Because of the complexity of the mixed boundary conditions, an analytical solution of eq 3a in terms of the original coordinates $\underline{x}$ and $\underline{y}$ was not attempted. The Schwarz-Christoffel transformation was used to map the original physical problem into an equivalent system from which the amount of air flow can readily be evaluated for various geometrical arrangements.

Mathematical analysis

From the Schwarz-Christoffel theorem (App. A), the α plane of Figure 1 is related to the β plane of Figure 2 by

$$\alpha = C_2 \int_0^{\beta} \frac{1}{(1 - \beta^2 k^{*2} sn^2 \tau)} \left(\frac{1 - \beta^2}{1 - k^{*2} \beta^2} \right)^{\frac{1}{2}} d\beta \qquad (4)$$

where τ is the real coordinate of the point E, F in Figure 3.

By substituting (Nehari, 1952)

$$\beta = sn\, \gamma \qquad (5)$$

in eq 4, which transforms Figure 2 into Figure 3, we show in Appendix A that the integral for α can be evaluated in terms of elliptic functions

$$a = C_2\left[\gamma - \frac{\mathrm{dn}\tau}{k^{*2}\,\mathrm{sn}\tau\,\mathrm{cn}\tau}\left\{\gamma Z(\tau) - \tfrac{1}{2}\log\frac{\theta(\gamma-\tau)}{\theta(\gamma+\tau)}\right\}\right] \tag{6}$$

where cn and dn are Jacobian elliptic functions; Z is the Jacobian zeta function and $\theta(u)$ is the theta function defined as (Wilson, 1958)

$$\sum_{n=-\infty}^{n=\infty}(-1)^n \exp\left(-\frac{\pi K' n^2}{K}\right)\exp\left(\frac{in\pi u}{K}\right).$$

As derived in Appendix B, d_ℓ, d_t, and b can be obtained from eq 6 and expressed as

$$d_\ell = \frac{C_2\,\pi\,\mathrm{dn}\tau}{2k^{*2}\,\mathrm{sn}\tau\,\mathrm{cn}\tau} \tag{7a}$$

$$d_t = C_2\left[\frac{K'Z(\tau)\,\mathrm{dn}\tau}{k^{*2}\,\mathrm{sn}\tau\,\mathrm{cn}\tau} - \frac{\mathrm{dn}\tau}{k^{*2}\,\mathrm{sn}\tau\,\mathrm{cn}\tau}\left(\frac{\pi\tau}{2K}\right)\right] \tag{7b}$$

and

$$b = C_2\left(-K + \frac{KZ(\tau)\,\mathrm{dn}\tau}{k^{*2}\,\mathrm{sn}\tau\,\mathrm{cn}\tau}\right) \tag{7c}$$

respectively.

Defining $R_1 = d_\ell/b$ and $R_2 = d_t/b$, we get from eq 7a, 7b and 7c

$$R_1 = \frac{(\pi/2)\,\mathrm{dn}\tau}{K[k^{*2}\,\mathrm{sn}\tau\,\mathrm{cn}\tau - Z(\tau)\,\mathrm{dn}\tau]} \tag{8a}$$

$$R_2 = \frac{-K'[k^{*2}\,\mathrm{sn}\tau\,\mathrm{cn}\tau - Z(\tau)\,\mathrm{dn}\tau] + (\pi\tau/2K)\,\mathrm{dn}\tau}{K[k^{*2}\,\mathrm{sn}\tau\,\mathrm{cn}\tau - Z(\tau)\,\mathrm{dn}\tau]}\,. \tag{8b}$$

Similarly the expression for $R_3 = d_c/d_t$, as shown in Appendix C, is

$$R_3 = 1 - \left\{\frac{\lambda[k^{*2}\,\mathrm{sn}\tau\,\mathrm{cn}\tau - Z(\tau)\,\mathrm{dn}\tau] - \frac{1}{2}\phi\,\mathrm{dn}\tau}{K'[k^{*2}\,\mathrm{sn}\tau\,\mathrm{cn}\tau - Z(\tau)\,\mathrm{dn}\tau] - (\pi\tau/2K)\,\mathrm{dn}\tau}\right\} \tag{8c}$$

where λ stands for the imaginary coordinate of point C in Figure 3 and ϕ represents the principal argument of $\theta(K + i\lambda - \tau)/\theta(K + i\lambda + \tau)$.

In conjunction with eq 8a and 8b, a computer program was written which furnished the data for Figures 4, 5, 6 and 7. The latter two figures were not prepared by just cross plotting from Figures 4 and 5 since in many parts of Figures 4 and 5 the curves are either too flat or too steep to obtain reliable relations among R_1, R_2 and τ/K for a given k^{*2}. Therefore, to prepare Figures 6 and 7 from Figures 4 and 5, R_1, R_2 and τ/K values were first tabulated for given values of k^{*2}; the computer program prepared for obtaining Figures 4 and 5 was then used again to get more exact values of R_1, R_2 and τ/K. It can be seen from Table I that the computed values of (R_1) and $(R_2)_{calc}$ are in close agreement with given R_1, R_2, for particular values of τ/K and k^{*2}. With these values of τ/K and k^{*2} corresponding to a given set of R_1 and R_2, the unique value of λ for a given R_3 is found from eq 8c by the method of trial and error. By using this λ, the coordinate of point C in the β plane, σ, is calculated from eq 5:

$$\sigma = \mathrm{sn}(K + i\lambda).$$

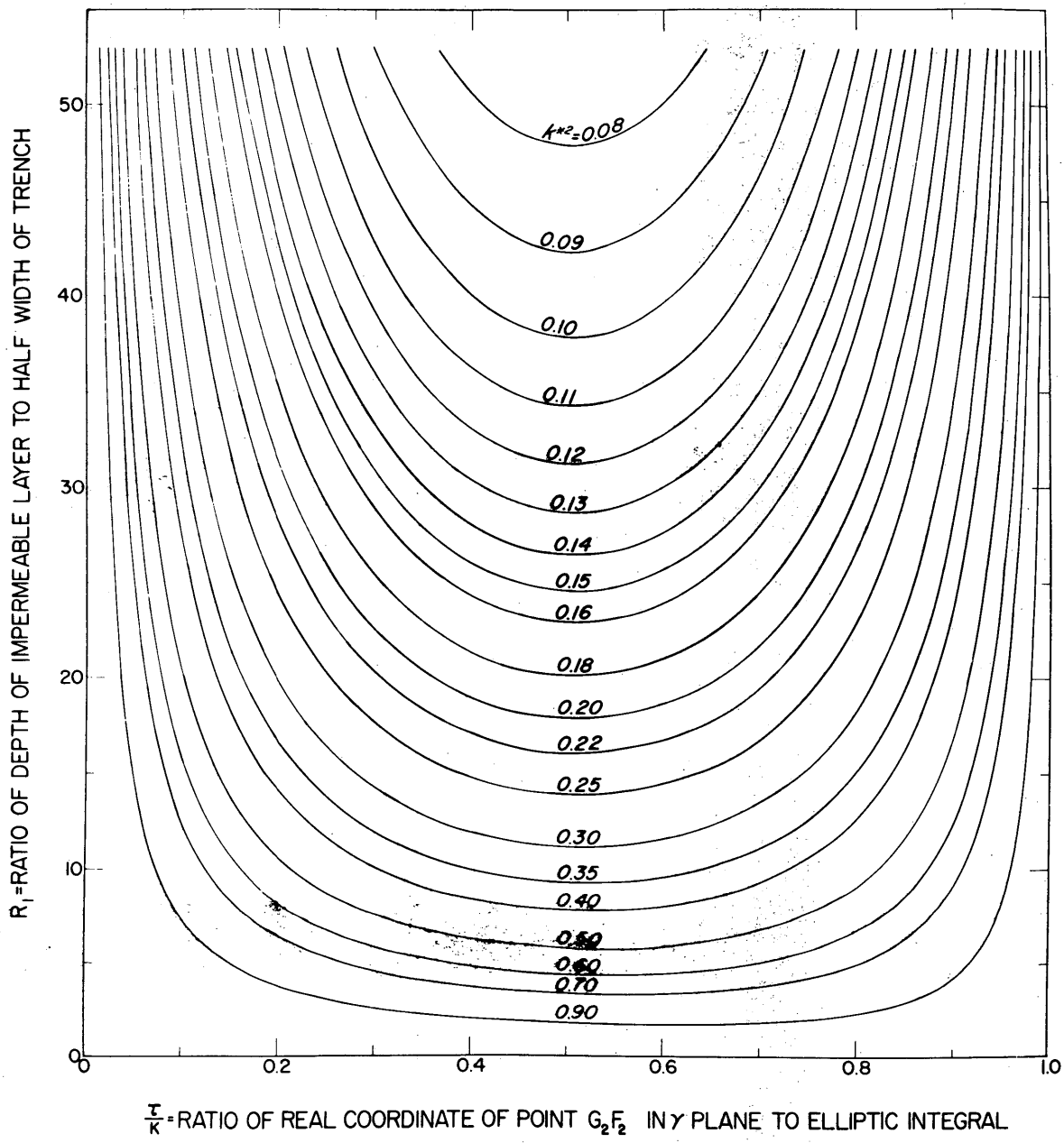

Figure 4. Relationship between R_1 and τ/K.

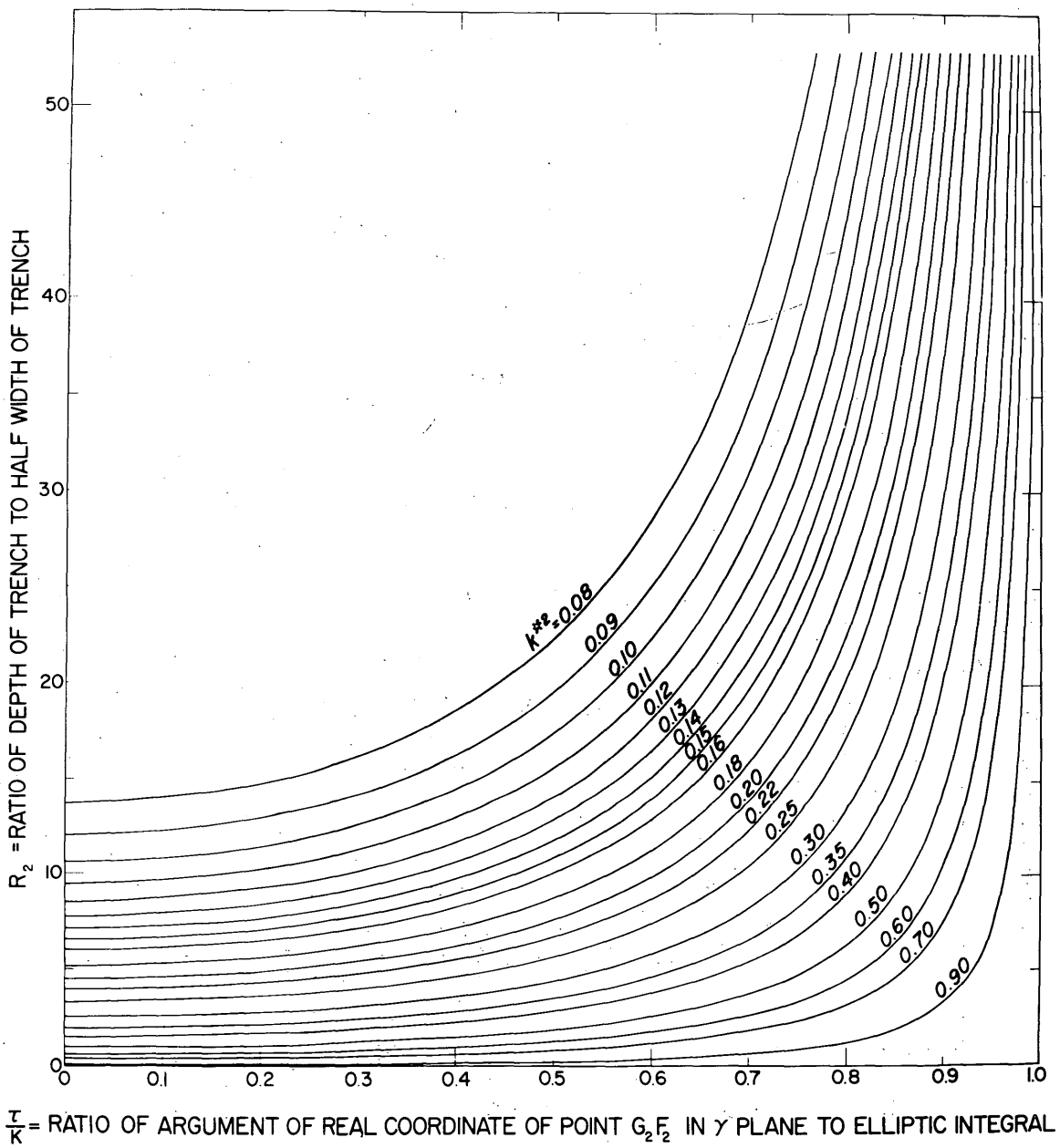

Figure 5. Relationship between R_2 and τ/K.

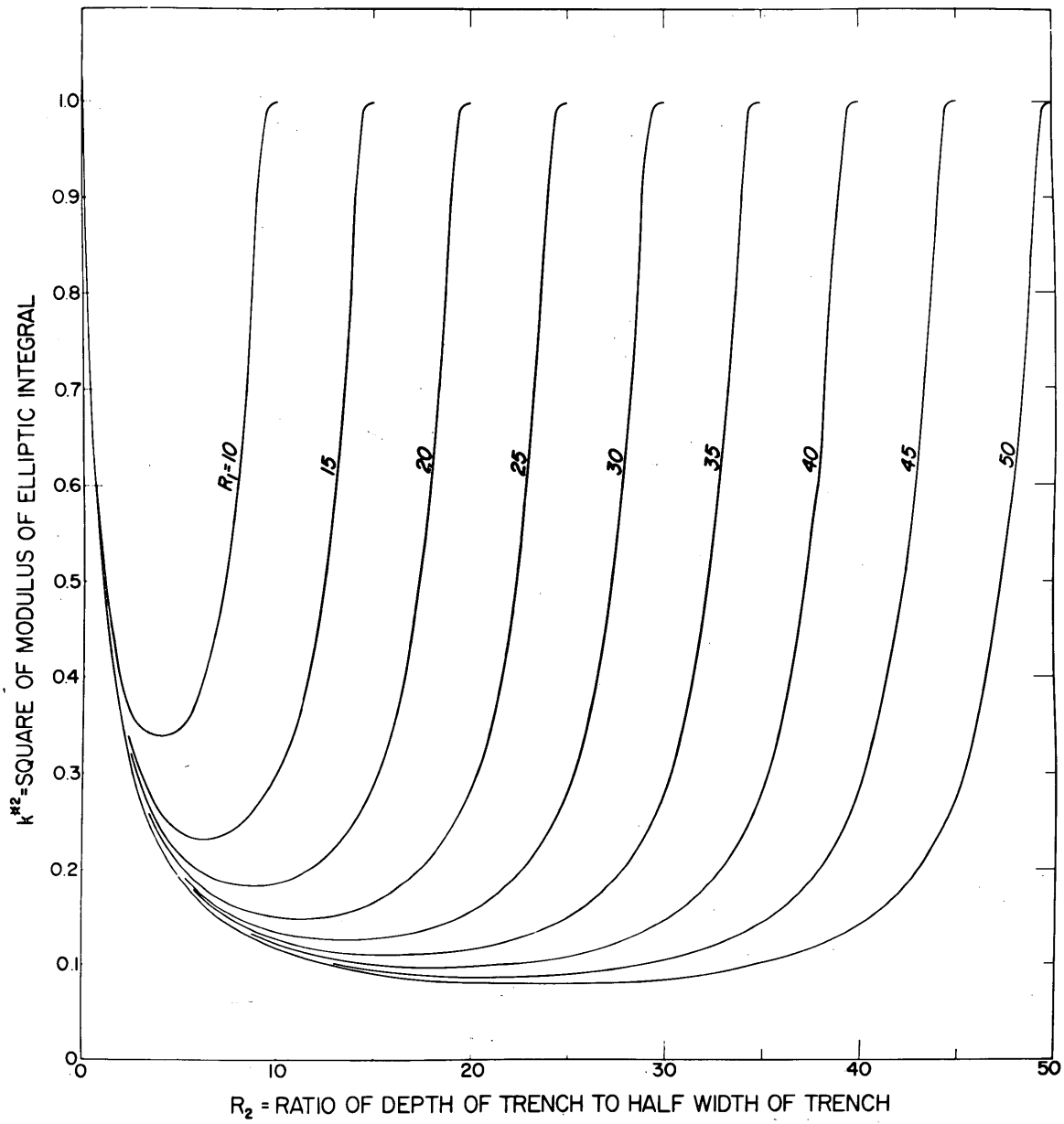

Figure 6. Relationship between k^{*2} and R_2.

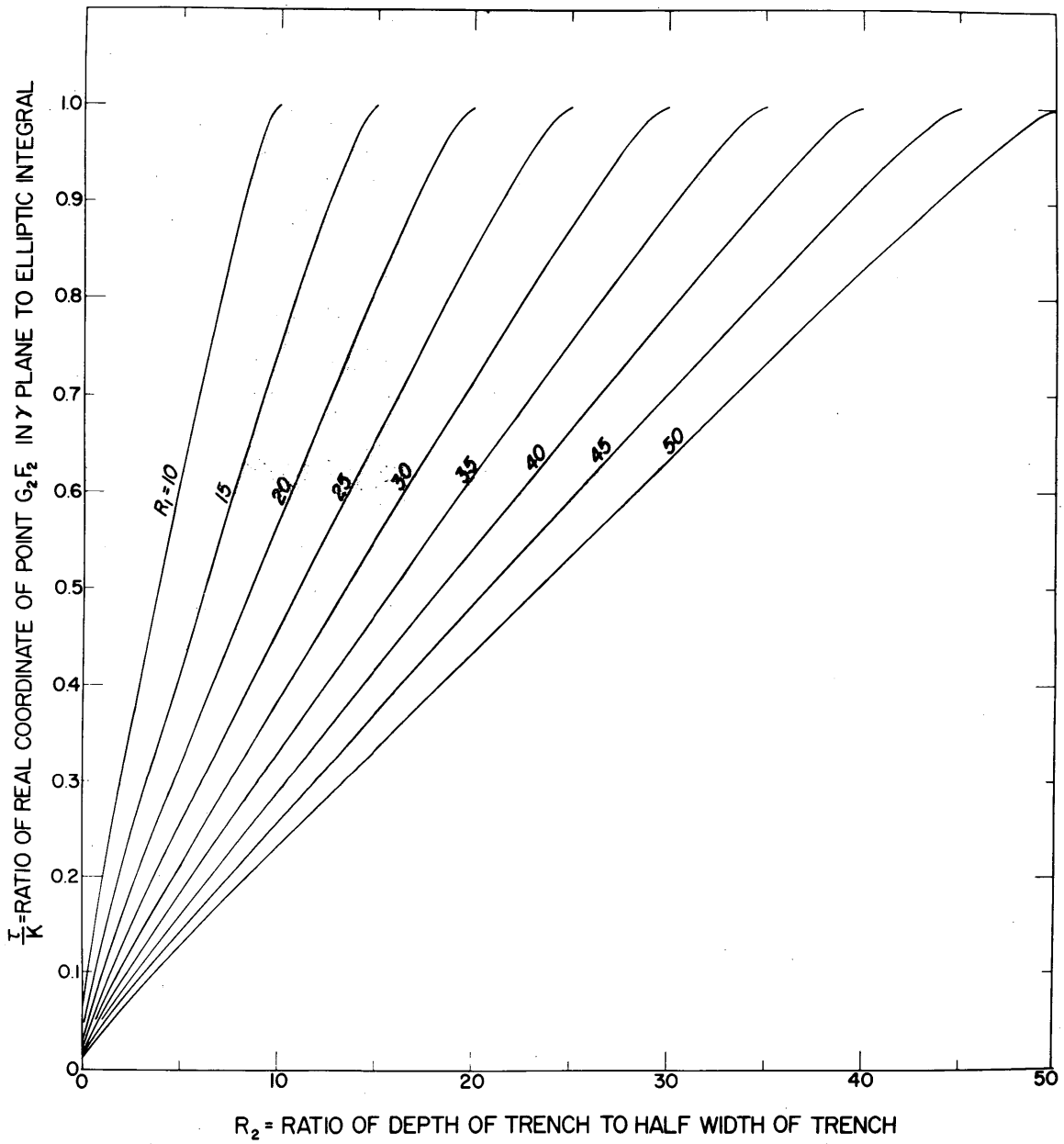

Figure 7. Relationship between τ/K and R_2 .

Table I. Evaluation of k^{*2} and τ for a given set of R_1 and R_2.

R_1	R_2	τ/K	k^{*2}	$sn\tau$	$cn\tau$	$dn\tau$	$Z(\tau)$	K	K'	$(R_1)_{calc}$	$(R_2)_{calc}$
50	40	0.830	0.143	0.96707	0.25450	0.93073	0.01859	1.63197	2.41113	50.0689	40.07947
	30	0.631	0.083	0.84202	0.53945	0.97013	0.01934	1.60501	2.66618	50.13929	29.97673
	20	0.432	0.079	0.63548	0.77211	0.98392	0.01974	1.60328	2.68956	49.84367	19.85493
	10	0.230	0.115	0.36295	0.93181	0.99240	0.01982	1.61913	2.51256	50.07943	9.96648
40	32	0.835	0.179	0.96962	0.24460	0.91198	0.02278	1.64919	2.30778	40.06323	32.05345
	24	0.636	0.103	0.84753	0.53074	0.96230	0.02393	1.61377	2.56424	40.20208	23.97955
	16	0.441	0.097	0.64822	0.76145	0.97941	0.02450	1.61112	2.59248	39.97918	16.02170
	8	0.235	0.140	0.37269	0.92795	0.99023	0.02479	1.63058	2.42093	39.96081	7.90608
30	24	0.842	0.238	0.97315	0.23017	0.88012	0.02938	1.67930	2.17859	29.98860	23.95308
	18	0.647	0.137	0.85869	0.51249	0.94815	0.03153	1.62918	2.43099	30.07744	17.96795
	12	0.449	0.127	0.66093	0.75045	0.97186	0.03249	1.62458	2.46622	29.91553	11.9140
	6	0.247	0.176	0.39409	0.91907	0.98624	0.03287	1.64772	2.31552	30.01588	6.00863
20	16	0.854	0.349	0.97882	0.20472	0.81586	0.04080	1.74372	2.00885	20.0543	15.97435
	12	0.667	0.203	0.87820	0.47830	0.91839	0.04576	1.66114	2.25045	20.08397	12.04124
	8	0.470	0.182	0.69140	0.72247	0.95551	0.04770	1.65087	2.30019	20.05616	8.03308
	4	0.266	0.241	0.42926	0.90318	0.97754	0.04890	1.68091	2.17296	20.01607	4.03154
10	8	0.882	0.623	0.98966	0.14342	0.62435	0.06280	1.97522	1.76190	10.08816	8.00576
	6	0.709	0.388	0.91732	0.39814	0.82067	0.08310	1.76929	1.96275	9.91216	5.91838
	4	0.521	0.337	0.76399	0.64523	0.89627	0.09236	1.73619	2.02416	9.72950	3.90320
	2	0.310	0.394	0.51373	0.85795	0.94658	0.09495	1.77338	1.95610	10.00797	1.99943

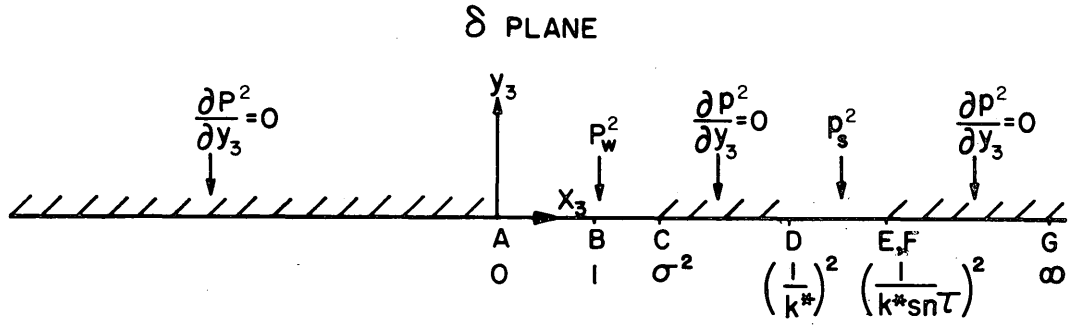

Figure 8. First quadrant of β plane mapped into upper half of δ plane.

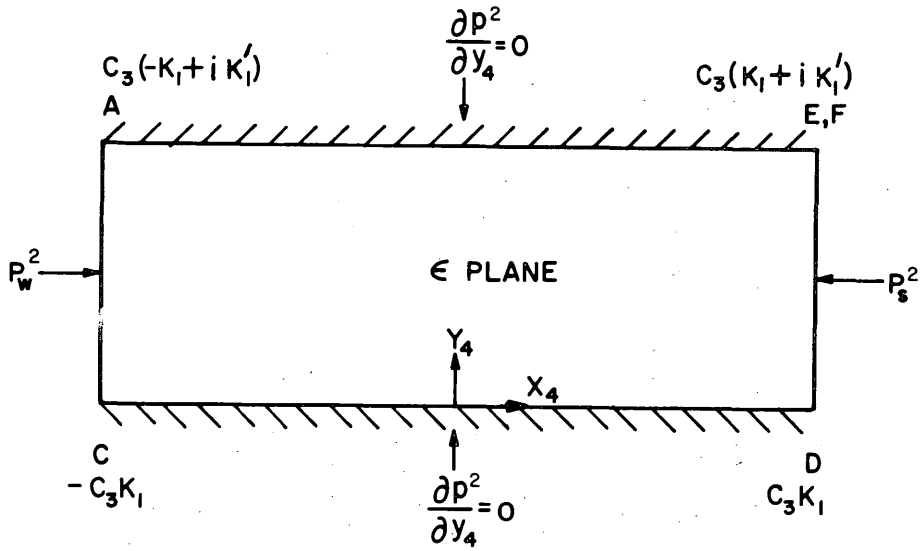

Figure 9. Figure 8 mapped into an equivalent linear system.

The complex function

$$\delta = \beta^2 \tag{9}$$

is then used to map the first quadrant of the β plane of Figure 2 onto the upper half of the δ plane of Figure 8. Since there is no flow across the line $x_1 = 0$ in Figure 2 due to symmetry, the appropriate boundary condition is shown to the left of point A in Figure 8.

With the application of the Schwarz-Christoffel theorem, Figure 8 can be transformed into Figure 9 (Bateman, 1944). The ratio $K_1'/2K_1$, which is the width to length ratio of the equivalent linear system indicated in Figure 9, can be obtained by solving the quadratic equation

$$\left[\left(\frac{1}{k^{*2}} - \sigma^2\right)\left(\frac{1}{k^{*2}\, sn^2\, \tau}\right)\right]k_1^{*2} - \left[\left(\frac{1}{k^{*2}} - \sigma^2\right) - \left(\sigma^2 + \frac{1}{k^{*2}} - \frac{1}{k^{*2} sn^2\, \tau}\right)\right] k_1^* +$$

$$+ \left(\frac{1}{k^{*2}} - \sigma^2\right)\left(\frac{1}{k^{*2}\, sn^2\, \tau}\right) = 0 \tag{10}$$

for k_1*. Values of K_1 and K_1' are found by interpolation from a table of elliptic integrals for k_1* less than unity (Hodgman, 1955). Table II shows the calculated values of $K_1'/2K_1$ for a given set of R_1, R_2 and various values of R_3. Figures 10 through 14 graphically indicate the relationship between $K_1'/2K_1$ and R_3 for a given R_1 using R_2 as parameter. Figures 15 through 19 are cross plots of Figures 10 through 14; values of $K_1'/2K_1$ for $d_t/d_\ell = 1.0$ were obtained from a previous study neglecting the effect of trench width (Yen and Fisher, 1963).

From Figure 9, the mass flow rate per unit length of trench is

$$Q = -2(K_1')\left(\frac{k}{\mu}\right)(\rho)\frac{dp}{dx}. \tag{11}$$

The factor 2 in eq 11 was introduced because only half of the symmetrical trench was considered in the above analysis. For ideal gas, $\rho = p/RT$, eq 11 becomes

$$Q = -2(K_1')\left(\frac{k}{\mu}\right)\left(\frac{1}{2RT}\right)\frac{dp^2}{dx} \tag{12}$$

or

$$Q = 2\left(\frac{K_1'}{2K_1}\right)\left(\frac{k}{\mu}\right)\left(\frac{1}{2RT}\right)(p_s^2 - p_w^2). \tag{12a}$$

Finally, we have

$$Q = 2\left(\frac{K_1'}{2K_1}\right)\left(\frac{k}{\mu}\right)(\rho_{avg})(p_s - p_w) \tag{12b}$$

by writing $\rho_{avg} = (p_s + p_w)/2RT$.

Discussion of results

Computed values of $K_1'/2K_1$ for various R_1's are graphically shown in Figures 15 through 19 using R_2/R_1 as parameter. For a given set of p_s and p_w values, the following conclusions can be drawn from these figures:

(1) For a constant value of R_1 and R_3, values of $K_1'/2K_1$ increase as R_2/R_1 decreases. Hence, if d_ℓ and $\underline{b}$ are fixed and the same percentage of the trench is cased, the mass flux will decrease continuously as the bottom of the trench approaches the impermeable layer. The effect of d_t on the value of $K_1'/2K_1$ is clearly illustrated by the following example: For the case of $R_1 = 30$, $R_2/R_1 = 0.4$, and $R_3 = 0.4$, $K_1'/2K_1 = 1.45$ from Figure 16. Doubling the depth of the trench while maintaining d_c, d_ℓ, and $\underline{b}$ unchanged, we have $R_1 = 30$, $R_2/R_1 = 0.80$, $R_3 = 0.2$ and $K_1'/2K_1 = 1.73$. Therefore, increasing d_t by a factor of 2 causes only a slight increase of $K_1'/2K_1$.

(2) For constant values of R_2/R_1 and R_1, $K_1'/2K_1$ decreases as R_3 increases. Hence, as expected, with a given d_ℓ and a specified trench size, the flow decreases as d_c increases.

(3) $K_1'/2K_1$ remains essentially constant for given values of R_2/R_1 and R_3. Physically this clearly indicates that, for values of R_1 ranging from 10 to 50, the variation in trench width produces only a negligible effect on $K_1'/2K_1$ for constant values of d_ℓ, d_t and d_c.

The magnitude of the error in $K_1'/2K_1$ introduced by not considering the trench width can be obtained by comparing Figures 15 through 19 with Figure 8 of our previous paper (Yen and Fisher, 1963). Consider the case $R_2/R_1 = 0.25$ and $R_1 = 30$; Table III shows the effect of half trench width $\underline{b}$ on the value of $K_1'/2K_1$ for various values of R_3.

As shown in the table, the effect of trench width on $K_1'/2K_1$ decreases as R_3 decreases. However, without exception, the flow through the bottom of the trench contributes significantly to the total flow. For instance, with $R_3 = 0.20$ (20% of the trench

cased), the error introduced in $K_1'/2K_1$ by not including the trench width still amounts to about 16%. In any practical analysis it is concluded that the trench width effect should be considered.

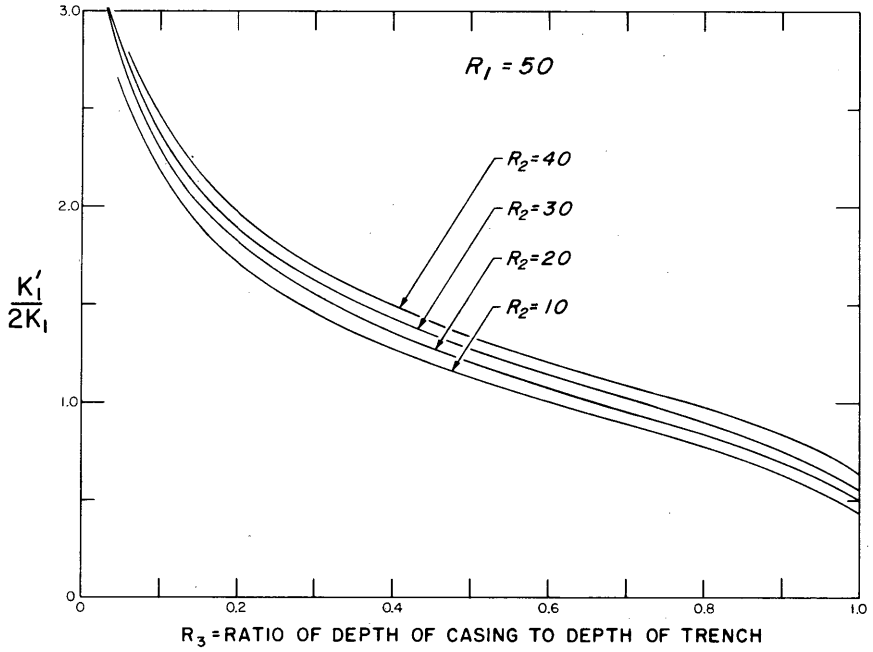

Figure 10. Relationship between $K_1'/2K_1$ and R_3, $R_1 = 50$.

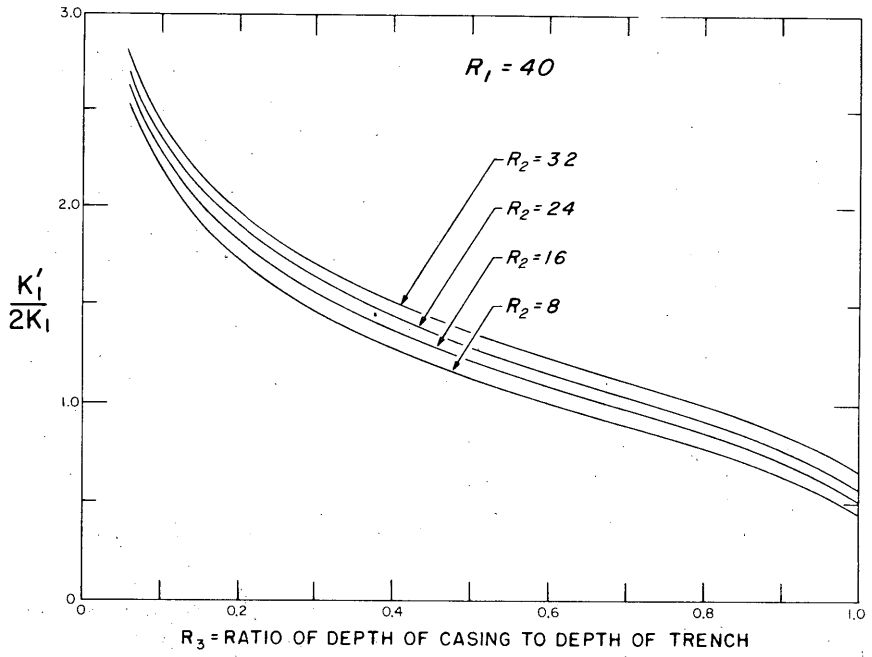

Figure 11. Relationship between $K_1'/2K_1$ and R_3, $R_1 = 40$.

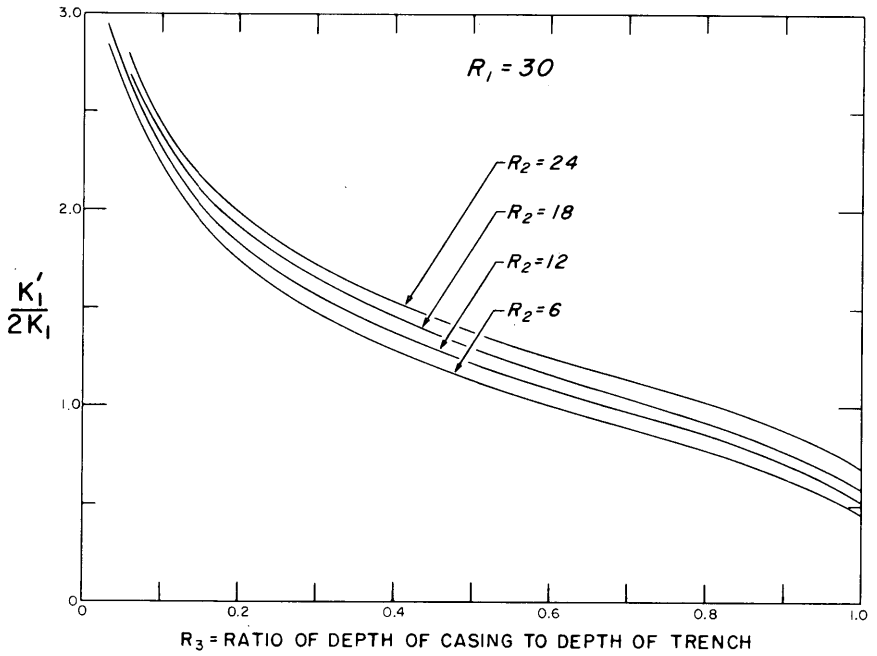

Figure 12. Relationship between $K_1'/2K_1$ and R_3, $R_1 = 30$.

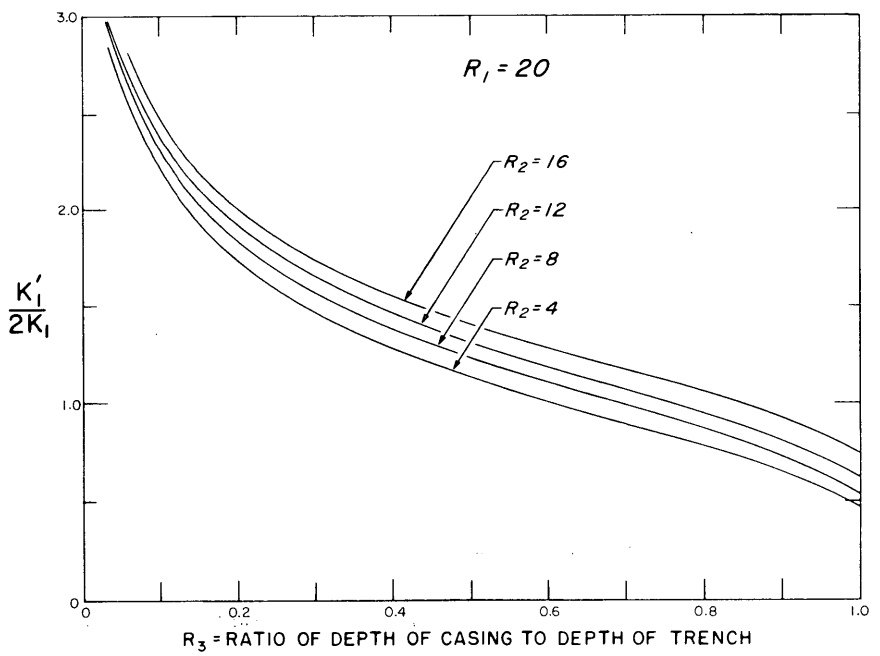

Figure 13. Relationship between $K_1'/2K_1$ and R_3, $R_1 = 20$.

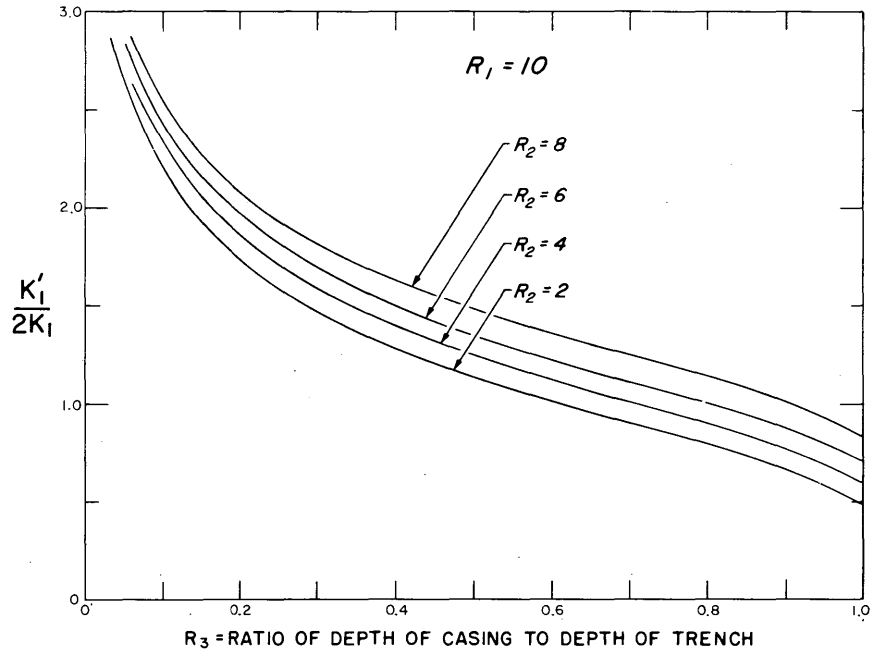

Figure 14. Relationship between $K_1'/2K_1$ and R_3, $R_1 = 10$.

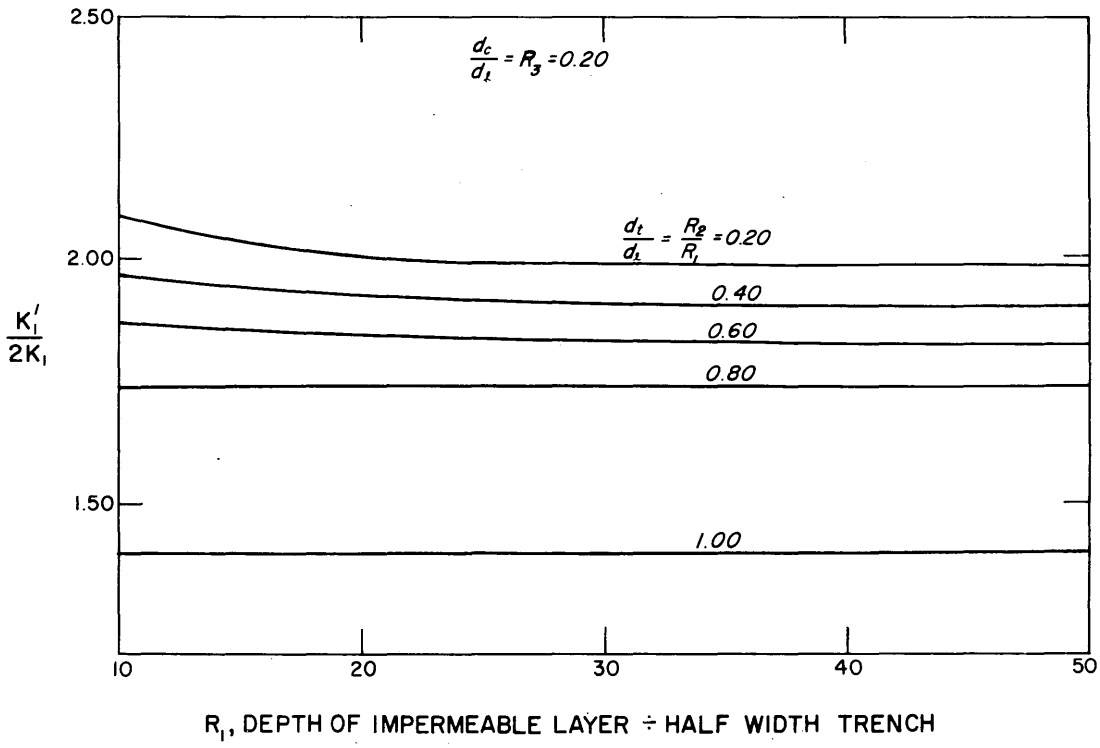

Figure 15. Relationship between $K_1'/2K_1$ and R_1 for $R_3 = 0.20$.

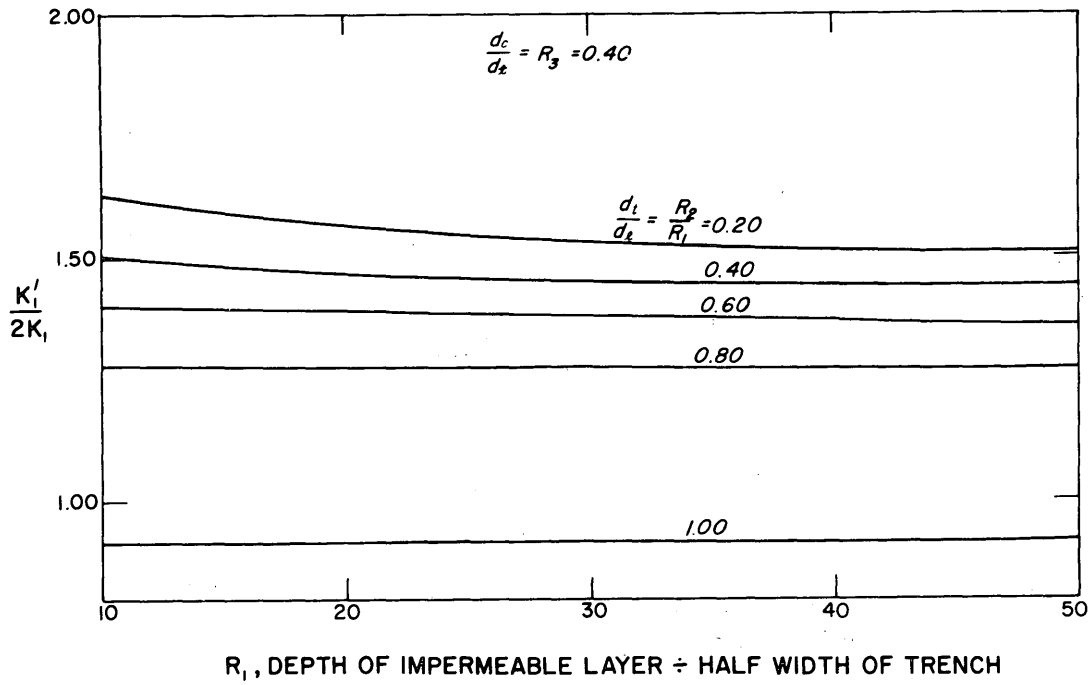

Figure 16. Relationship between $K_1'/2K_1$ and R_1 for $R_3 = 0.40$.

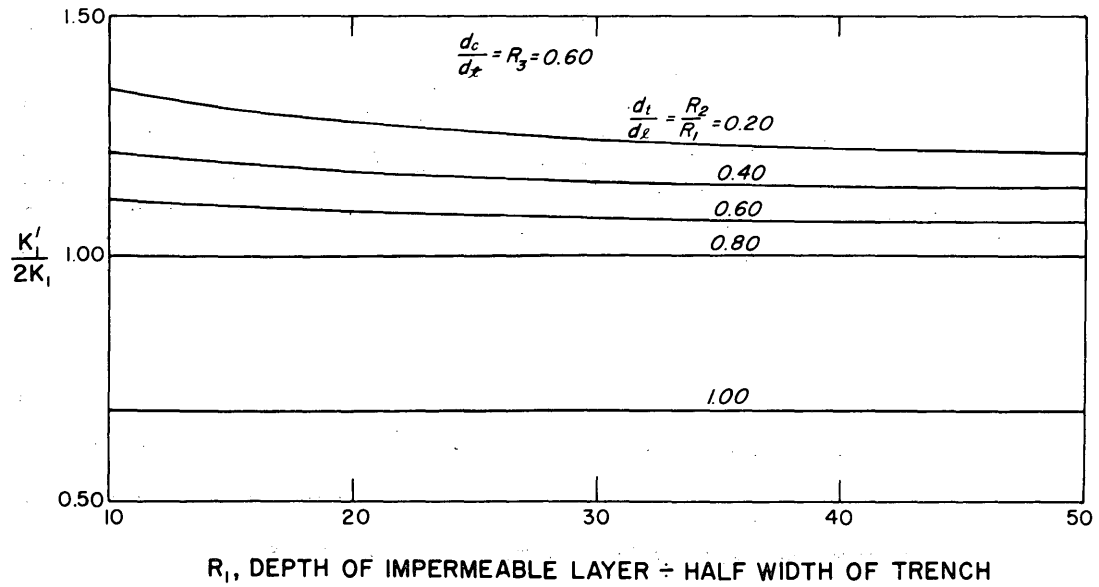

Figure 17. Relationship between $K_1'/2K_1$ and R_1 for $R_3 = 0.60$.

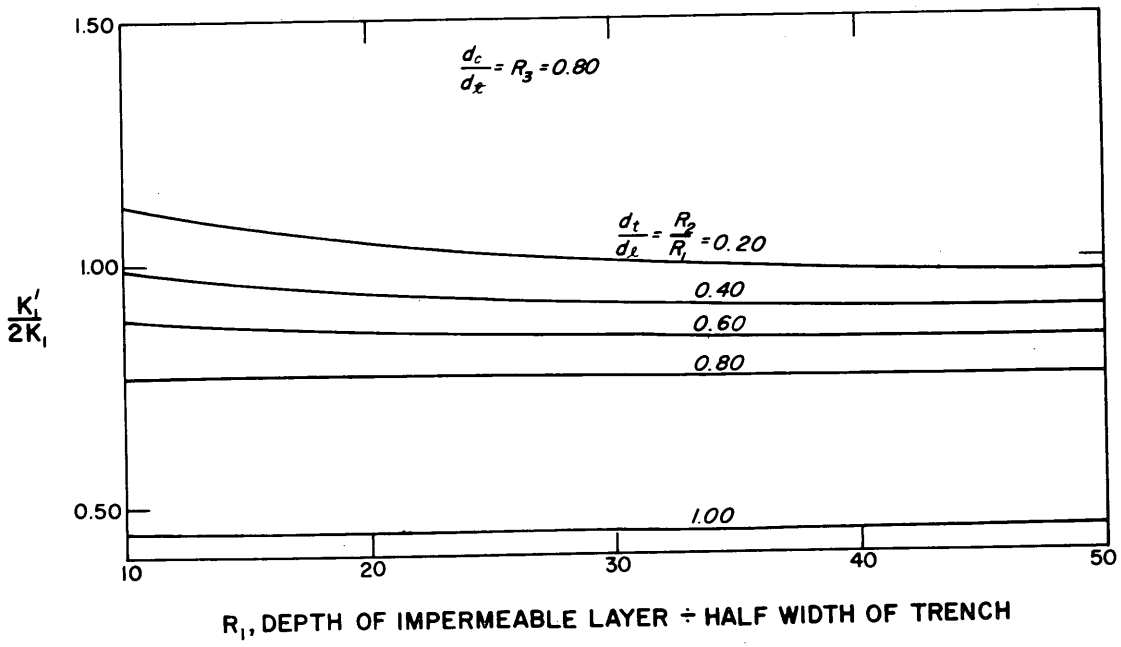

Figure 18. Relationship between $K_1'/2K_1$ and R_1 for $R_3 = 0.80$.

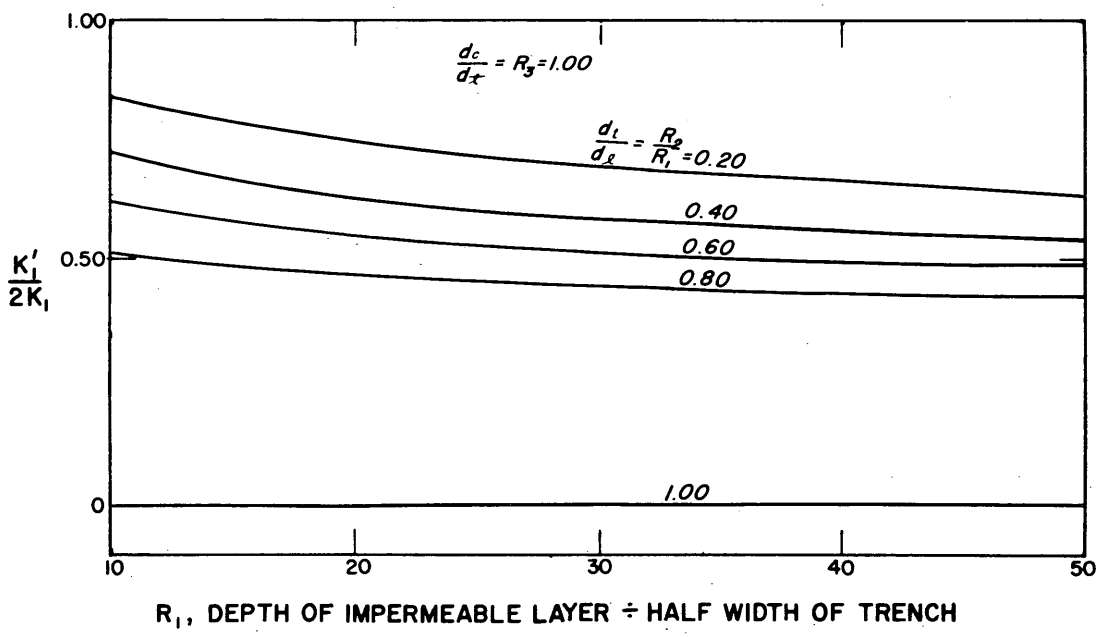

Figure 19. Relationship between $K_1'/2K_1$ and R_1 for $R_3 = 1.00$.

Table II. Evaluation of $K_1'/2K_1$ for given set of R_1 and R_2 as function of R_3.

a) $R_1 = 50$

$R_2 = 40$		$R_2 = 30$		$R_2 = 20$		$R_2 = 10$	
R_3	$K_1'/2K_1$	R_3	$K_1'/2K_1$	R_3	$K_1'/2K_1$	R_3	$K_1'/2K_1$
1.000	0.425	1.000	0.490	1.000	0.540	1.000	0.630
0.950	0.565	0.942	0.655	0.946	0.690	0.944	0.770
0.893	0.650	0.901	0.715	0.906	0.770	0.904	0.835
0.857	0.695	0.855	0.775	0.848	0.850	0.844	0.910
0.807	0.751	0.810	0.830	0.805	0.910	0.799	0.955
0.749	0.818	0.752	0.895	0.754	0.970	0.743	1.025
0.709	0.863	0.700	0.955	0.694	1.010	0.704	1.090
0.643	0.935	0.650	1.020	0.654	1.080	0.650	1.140
0.599	0.992	0.591	1.090	0.610	1.150	0.601	1.200
0.555	1.052	0.547	1.145	0.551	1.220	0.546	1.275
0.496	1.125	0.490	1.230	0.499	1.280	0.502	1.350
0.453	1.190	0.450	1.285	0.441	1.360	0.445	1.430
0.391	1.290	0.399	1.365	0.402	1.450	0.393	1.500
0.354	1.355	0.352	1.450	0.353	1.530	0.345	1.590
0.302	1.460	0.298	1.560	0.297	1.650	0.292	1.705
0.256	1.570	0.242	1.705	0.240	1.770	0.245	1.840
0.202	1.730	0.195	1.840	0.193	1.910	0.198	1.985
0.158	1.870	0.157	1.980	0.155	2.045	0.159	2.125
0.106	2.150	0.095	2.310	0.109	2.365	0.096	2.350
0.048	2.670	0.057	2.650	0.055	2.695	0.058	2.795
0.016		0.034	3.015	0.033	3.030	0.035	

b) $R_1 = 40$

$R_2 = 32$		$R_2 = 24$		$R_2 = 16$		$R_2 = 8$	
1.000	0.430	1.000	0.495	1.000	0.560	1.000	0.655
0.947	0.575	0.945	0.660	0.940	0.725	0.942	0.795
0.901	0.650	0.907	0.720	0.899	0.785	0.900	0.855
0.851	0.710	0.847	0.790	0.853	0.842	0.855	0.915
0.800	0.760	0.801	0.845	0.790	0.925	0.796	0.985
0.742	0.830	0.742	0.910	0.758	0.960	0.744	1.050
0.692	0.875	0.700	0.970	0.694	1.035	0.709	1.095
0.654	0.925	0.651	1.020	0.650	1.090	0.642	1.175
0.600	0.990	0.591	1.090	0.602	1.150	0.598	1.230
0.547	1.055	0.548	1.150	0.548	1.215	0.551	1.290
0.494	1.120	0.491	1.230	0.504	1.280	0.500	1.365
0.443	1.210	0.450	1.290	0.447	1.370	0.442	1.450
0.394	1.285	0.399	1.375	0.395	1.450	0.402	1.510
0.349	1.370	0.352	1.450	0.347	1.540	0.340	1.625
0.297	1.475	0.298	1.570	0.295	1.650	0.298	1.730
0.242	1.610	0.242	1.710	0.247	1.770	0.240	1.870
0.196	1.745	0.195	1.845	0.199	1.910	0.194	2.000
0.158	1.885	0.157	1.990	0.160	2.045	0.156	2.140
0.096	2.210	0.095	2.310	0.096	2.370	0.109	2.370
0.058	2.535	0.057	2.640	0.058	2.700	0.055	2.805

c) $R_1 = 30$

$R_2 = 24$		$R_2 = 18$		$R_2 = 12$		$R_2 = 6$	
1.000	0.450	1.000	0.520	1.000	0.540	1.000	0.690
0.944	0.590	0.947	0.670	0.946	0.730	0.948	0.810
0.906	0.640	0.900	0.730	0.908	0.790	0.910	0.870
0.844	0.720	0.854	0.790	0.850	0.870	0.853	0.940
0.791	0.775	0.791	0.870	0.807	0.910	0.795	1.010
0.745	0.830	0.756	0.910	0.756	0.975	0.744	1.070
0.696	0.880	0.708	0.960	0.694	1.050	0.709	1.110
0.643	0.940	0.650	1.030	0.651	1.095	0.644	1.190
0.604	0.990	0.590	1.100	0.604	1.160	0.601	1.240
0.550	1.055	0.547	1.150	0.552	1.230	0.555	1.300
0.497	1.120	0.504	1.210	0.492	1.310	0.505	1.370
0.446	1.210	0.449	1.300	0.450	1.370	0.447	1.450
0.397	1.285	0.398	1.380	0.398	1.450	0.393	1.550
0.340	1.390	0.351	1.465	0.350	1.550	0.345	1.630
0.300	1.470	0.297	1.575	0.295	1.660	0.291	1.750
0.244	1.610	0.241	1.710	0.248	1.770	0.244	1.860
0.198	1.750	0.195	1.850	0.200	1.910	0.197	2.000
0.160	1.880	0.157	1.990	0.141	2.140	0.158	2.150
0.097	2.205	0.095	2.320	0.099	2.370	0.095	2.470
0.056	2.530	0.057	2.640	0.060	2.690	0.057	2.800
0.035	2.850	0.034	2.970	0.030		0.035	

Table II (Cont'd). Evaluation of $K_1'/2K_1$ for given set of R_1 and R_2 as function of R_3.

d) $R_1 = 20$

$R_2 = 16$		$R_2 = 12$		$R_2 = 8$		$R_2 = 4$	
R_3	$K_1'/2K_1$	R_3	$K_1'/2K_1$	R_3	$K_1'/2K_1$	R_3	$K_1'/2K_1$
1.000	0.470	1.000	0.550	1.000	0.620	1.000	0.740
0.957	0.575	0.942	0.690	0.950	0.750	0.943	0.865
0.900	0.660	0.903	0.750	0.893	0.830	0.901	0.920
0.853	0.715	0.844	0.820	0.846	0.890	0.842	0.990
0.805	0.770	0.800	0.870	0.803	0.940	0.800	1.050
0.759	0.820	0.743	0.930	0.752	1.000	0.750	1.095
0.696	0.890	0.703	0.975	0.691	1.070	0.693	1.160
0.643	0.940	0.658	1.030	0.649	1.120	0.654	1.210
0.604	0.955	0.606	1.090	0.603	1.180	0.604	1.275
0.550	1.060	0.547	1.165	0.553	1.240	0.559	1.330
0.497	1.130	0.504	1.230	0.493	1.320	0.500	1.410
0.445	1.210	0.449	1.300	0.451	1.390	0.449	1.490
0.397	1.290	0.398	1.390	0.398	1.470	0.396	1.570
0.351	1.370	0.351	1.470	0.350	1.560	0.347	1.660
0.299	1.475	0.297	1.580	0.295	1.670	0.292	1.770
0.244	1.610	0.241	1.720	0.248	1.790	0.245	1.890
0.197	1.750	0.194	1.860	0.200	1.925	0.197	1.990
0.159	1.885	0.156	1.995	0.141	2.140	0.159	2.170
0.096	2.210	0.095	2.320	0.099	2.360	0.096	2.500
0.058	2.530	0.057	2.645	0.060	2.660	0.058	2.820
0.035	2.850	0.034	2.975	0.030	3.000		

e) $R_1 = 10$

$R_2 = 8$		$R_2 = 6$		$R_2 = 4$		$R_2 = 2$	
1.000	0.510	1.000	0.615	1.000	0.710	1.000	0.840
0.954	0.600	0.945	0.725	0.942	0.830	0.946	0.950
0.894	0.675	0.907	0.775	0.902	0.880	0.905	1.005
0.844	0.735	0.852	0.840	0.843	0.950	0.847	1.070
0.795	0.785	0.791	0.905	0.801	0.990	0.806	1.115
0.757	0.830	0.759	0.935	0.751	1.050	0.759	1.170
0.693	0.895	0.696	1.010	0.692	1.120	0.705	1.230
0.640	0.955	0.651	1.055	0.652	1.160	0.643	1.305
0.600	1.010	0.601	1.120	0.608	1.210	0.603	1.350
0.546	1.070	0.542	1.190	0.551	1.285	0.560	1.400
0.493	1.145	0.500	1.250	0.499	1.355	0.504	1.475
0.442	1.220	0.444	1.330	0.442	1.440	0.456	1.550
0.393	1.300	0.393	1.410	0.403	1.500	0.401	1.630
0.348	1.380	0.346	1.500	0.341	1.605	0.351	1.725
0.296	1.485	0.293	1.610	0.299	1.705	0.296	1.830
0.241	1.650	0.247	1.725	0.242	1.845	0.248	1.950
0.195	1.760	0.200	1.860	0.195	1.980	0.200	2.090
0.157	1.900	0.141	2.090	0.157	2.120	0.141	2.320
0.095	2.220	0.099	2.310	0.094	2.445	0.099	2.545
0.057	2.550	0.060	2.630	0.057	2.820	0.060	2.870
0.034	2.870	0.030		0.034			

Table III. Effect of trench width on values of $K_1'/2K_1$ for the case $R_2/R_1 = 0.25$ and $R_1 = 30$.

R_3	$K_1'/2K_1$ (Fig. 15-19)	$K_1'/2K_1$ (Fig. 8, Yen and Fisher, 1963)
0.20	1.97	1.66
0.40	1.51	1.21
0.60	1.22	0.92
0.80	0.98	0.66
1.00	0.66	0.00

REFERENCES

Bateman, H. (1944) Partial differential equations of mathematical physics. New York: Dover Publications, p. 302-303.

Carter, F. W. (1926) The magnetic field of the dynamo-electric machine, Journal of the Institution of Electrical Engineers, vol. 64, no. 359, p. 1115-1138.

Hodgman, C. D. (1955) Handbook of chemistry and physics. Cleveland: Chemical Rubber Publishing Company.

Nehari, Z. (1952) Conformal mapping. New York: McGraw-Hill Book Company, p. 280-299.

Wilson, E. B. (1958) Advanced calculus. New York: Dover Publications, p. 467-469.

Yen, Yin-Chao and Don Fisher (1963) On the isothermal flow of air into a rectangular snow trench, Journal of Geophysical Research, vol. 68, no. 24, p. 6475-6480. Also USA CRREL Research Report 144, Flow of air into a partially-cased snow trench.

APPENDIX A: DERIVATION OF EQUATION 6

Using the technique developed by Carter (1926), the transformation required to map Figure 1 into Figure 2 is

$$d\alpha = C_1 \frac{d\beta}{\left(\beta - \frac{1}{k^* \, sn\tau}\right)\left(\beta + \frac{1}{k^* \, sn\tau}\right)(\beta-1)^{-\frac{1}{2}}(\beta+1)^{-\frac{1}{2}}\left(\beta - \frac{1}{k^*}\right)^{\frac{1}{2}}\left(\beta + \frac{1}{k^*}\right)^{\frac{1}{2}}} =$$

$$= C_1 \frac{(1 - \beta^2)^{\frac{1}{2}} (-k^{*3} \, sn^2 \tau)}{(1 - k^{*2} \beta^2)^{\frac{1}{2}} (1 - k^{*2} \beta^2 \, sn^2 \tau)} \, d\beta$$

or

$$\alpha = C_2 \int_0^{\beta} \frac{(1 - \beta^2)^{\frac{1}{2}}}{(1 - k^{*2} \beta^2)^{\frac{1}{2}} (1 - k^{*2} \beta^2 \, sn^2 \tau)} \, d\beta . \tag{4}$$

With the substitution $\beta = sn\gamma$, the above expression becomes

$$\alpha = C_2 \int_0^{\gamma} \frac{cn^2 \gamma}{(1 - k^{*2} \, sn^2 \gamma \, sn^2 \tau)} \, d\gamma$$

which also can be written as

$$\alpha = C_2 \int_0^{\gamma} \left[1 - \frac{dn^2 \tau \, sn^2 \tau}{1 - k^{*2} \, sn^2 \gamma \, sn^2 \tau} \right] d\gamma$$

or

$$\alpha = C_2 \left[\gamma - \frac{dn\tau}{k^{*2} \, sn\tau \, cn\tau} \int_0^{\gamma} \frac{k^{*2} \, sn\tau \, cn\tau \, dn\tau \, sn^2 \gamma}{1 - k^{*2} \, sn^2 \tau \, sn^2 \gamma} \, d\gamma . \right.$$

Finally, it can be integrated as

$$\alpha = C_2 \left\{ \gamma - \frac{dn\tau}{k^{*2} \, sn\tau \, cn\tau} \left[\gamma Z(\tau) + \tfrac{1}{2} \log \frac{\theta(\gamma - \tau)}{\theta(\gamma + \tau)} \right] \right\} . \tag{6}$$

APPENDIX B: DERIVATION OF EQUATIONS 7a, 7b, and 7c

The depth of the impermeable layer, d_ℓ, is determined by substituting $(1/k^* \operatorname{sn}\tau)$ in the residue of the integral for α, namely

$$-id_\ell = -iC_1\pi\left(\frac{2}{k^* \operatorname{sn}\tau}\right)^{-1}\left(\frac{1}{k^{*2}\operatorname{sn}^2\tau} - 1\right)^{\frac{1}{2}}\left(\frac{1}{k^{*2}\operatorname{sn}^2\tau} - \frac{1}{k^{*2}}\right)^{-\frac{1}{2}}$$

therefore

$$d_\ell = \frac{C_1\pi k^* \operatorname{dn}\tau \operatorname{sn}\tau}{2 \operatorname{cn}\tau}$$

but

$$C_1 = \frac{-C_2}{k^{*3}\operatorname{sn}^2\tau}$$

hence

$$d_\ell = -\frac{C_2\,\pi \operatorname{dn}\tau}{2k^{*2}\operatorname{sn}\tau \operatorname{cn}\tau}\,. \tag{7a}$$

Since the coordinates of points G, G' in the α plane are $0 - i(d_\ell - d_t)$ and $0 + iK'$ in the γ plane, eq 6 gives

$$-i(d_\ell - d_t) = C_2\left\{iK'\left[1 - \frac{\operatorname{dn}\tau\, Z(\tau)}{k^{*2}\operatorname{sn}\tau \operatorname{cn}\tau}\right] - \frac{\operatorname{dn}\tau}{2k^{*2}\operatorname{sn}\tau \operatorname{cn}\tau}\log\left[\frac{\theta(iK' - \tau)}{\theta(iK' + \tau)}\right]\right\}$$

where the factor $\log \theta(iK' - \tau)/\theta(iK' + \tau)$ can be expressed in terms of

$$\log\left[\frac{\theta(iK' - \tau)}{\theta(iK' + \tau)}\right] = \log\left[\frac{\theta(\tau - iK')}{\theta(\tau + iK')}\right] = \log\left[-\exp\left(\frac{i\pi\tau}{K}\right)\right. =$$

$$= \log\left\{(-1)\,(-1)\exp\left[\pi i\left(\frac{\tau}{K} - 1\right)\right]\right\} = \left(\frac{\tau}{K} - 1\right) i\,(\pi \pm 2n_1\pi)$$

therefore

$$(d_\ell - d_c) = C_2\left\{-K'\left[1 - \frac{\operatorname{dn}\tau\, Z(\tau)}{k^{*2}\operatorname{sn}\tau \operatorname{cn}\tau}\right] + \frac{\operatorname{dn}\tau\,[(\tau/K) - 1\,](\pi \pm 2n_1\pi)}{2k^{*2}\operatorname{sn}\tau \operatorname{cn}\tau}\right\}.$$

Similarly, by applying eq 6 to point D, we get

$$-b + id_t = C_2\left\{(K + iK')\left[1 - \frac{Z(\tau)\operatorname{dn}\tau}{k^{*2}\operatorname{sn}\tau \operatorname{cn}\tau}\right] - \frac{\operatorname{dn}\tau}{2k^{*2}\operatorname{sn}\tau \operatorname{cn}\tau}\log\left[\frac{\theta(K + iK' - \tau)}{\theta(K + iK' + \tau)}\right]\right\}.$$

As indicated in the preceding analysis

$$\log\left[\frac{\theta(K + iK' - \tau)}{\theta(K + iK' + \tau)}\right] = \log\left[\frac{\theta(\tau - K - iK')}{\theta(\tau + K + iK')}\right] =$$

$$= \log\left[\exp\left(\frac{i\pi\tau}{K}\right)\right] = i\left(\frac{\pi\tau}{K} \pm 2n_2\,\pi\right)$$

therefore

$$-b + id_t = C_2\left\{(K + iK')\left[1 - \frac{Z(\tau)\operatorname{dn}\tau}{k^{*2}\operatorname{sn}\tau \operatorname{cn}\tau}\right] - \frac{\operatorname{dn}\tau}{2k^{*2}\operatorname{sn}\tau \operatorname{cn}\tau}\, i\left(\frac{\pi\tau}{K} \pm 2n_2\pi\right)\right\}.$$

Collecting real terms, we have

$$b = C_2\left[-K + \frac{KZ(\tau)\ dn\tau}{k^{*2}\ sn\tau\ cn\tau}\right]. \tag{7c}$$

Similarly, for imaginary terms, the following holds:

$$d_t = C_2\left[K' - \frac{K'Z(\tau)\ dn\tau}{k^{*2}\ sn\tau\ cn\tau} - \frac{dn\tau(\pi\tau/K \pm 2n_2\pi)}{2k^{*2}\ sn\tau\ cn\tau}\right].$$

Since the depth to the impermeable layer, d_ℓ, must be equal to the sum of the expressions given for $(d_\ell - d_t)$ and d_t, the depth of the trench, it is required that

$$\frac{C_2\pi\ dn\tau}{k^{*2}\ sn\tau\ cn\tau}\left[\pm n_1\left(\frac{\tau}{K} - 1\right) \pm n_2\right] \equiv 0$$

with the exception of the trivial case

$$\frac{C_2\pi\ dn\tau}{k^{*2}\ sn\tau\ cn\tau} \equiv 0.$$

The above condition can be identically satisfied if, and only if, $n_1 = n_2 \equiv 0$. Therefore,

$$d_t = C_2\left[K' - \frac{K'Z(\tau)\ dn\tau}{k^{*2}\ sn\tau\ cn\tau} - \frac{dn\tau}{k^{*2}\ sn\tau\ cn\tau}\left(\frac{\pi\tau}{2K}\right)\right]. \tag{7b}$$

APPENDIX C: DERIVATION OF EQUATION 8c

To obtain the expression for R_3 as shown in eq 8c in the text we substitute $K + i\lambda$ for γ in eq 6 which gives

$$-b + i(d_t - d_c) = C_2\left\{(K + i\lambda)\left[1 - \frac{dn\tau\ Z(\tau)}{k^{*2}\ sn\tau\ cn\tau}\right] - \right.$$

$$\left. - \frac{dn\tau}{2k^{*2}\ sn\tau\ cn\tau} \log\left[\frac{\theta(K + i\lambda - \tau)}{\theta(K + i\lambda + \tau)}\right]\right\}.$$

Equating imaginary terms, we have

$$d_t - d_c = C_2\left\{\lambda\left[1 - \frac{dn\tau\ Z(\tau)}{k^{*2}\ sn\tau\ cn\tau}\right] - \frac{\phi\ dn\tau}{2k^{*2}\ sn\tau\ cn\tau}\right\}$$

where ϕ is the principal argument of $\theta(K + i\lambda - \tau)/\theta(K + i\lambda + \tau)$. Dividing the above expression by d_t, transposing and replacing d_t with eq 7b, yields

$$R_3 = \frac{d_c}{d_t} = 1 - \left\{\frac{\lambda[k^{*2}\ sn\tau\ cn\tau - dn\tau\ Z(\tau)] - \frac{1}{2}\phi\ dn\tau}{K'[k^{*2}\ sn\tau\ cn\tau - Z(\tau)\ dn\tau] - (\pi\tau/2K)\ dn\tau}\right\}. \qquad (8c)$$

APPENDIX D: NOMENCLATURE

b	Half width of trench
C_1, C_2	Constants
d_c	Depth of casing
d_ℓ	Depth of impermeable layer
d_t	Depth of trench
k	Permeability
k^*	Modulus of $sn\tau$, $cn\tau$, $dn\tau$, $Z(\tau)$, K and K'
k_1^*	Modulus of K_1 and K_1'
K, K_1	Complete elliptic integrals with modulus k^* and k_1^* respectively
K', K_1'	Complete elliptic integrals with modulus $\sqrt{1-k^{*2}}$ and $\sqrt{1-k_1^{*2}}$ respectively
L, W	Length and width of linear system respectively
p_s, p_w	Pressure at trench surface and uncased trench wall respectively
R	Universal gas constant
R_1, R_2, R_3	Ratios of d_ℓ/b, d_t/b and d_c/d_t respectively
Q	Mass flow rate per unit time per unit length of trench
sn, cn, dn	Jacobian elliptic functions
T	Absolute temperature
x, y	Coordinates
Z	Jacobian zeta function
θ	Theta function
λ	Imaginary coordinate of point C in Figure 3
μ	Viscosity
ρ	Density
ρ_{avg}	Average air density defined as $(p_s + p_w)/2RT$
ϕ	Principal argument of $\theta(K + i\lambda - \tau)/\theta(K + i\lambda + \tau)$
τ	Real coordinates of points E, F in Figure 3